Investigation and Analysis of Angular Gyroscope Microelectromechanical Systems

Malinka Spasova Ivanova, Manuela Marinova Nakova, Ivan Nikolaev Ivanov and Krassimir Hristov Denishev

Abstract – **Gyroscope microelectromechanical systems (MEMS) are used in a wide spectrum of areas: aerospace industry, military, medicine, automotive industry and consumer electronics market with their dramatically reduced cost, size, and weight. This supposes a wide variety of design solutions, according to the gyroscope type, design style, MEMS technology, actuation mechanism, and coriolis sensor. The aim of this paper is to investigate, summarize and analyze the gyroscope MEMS design approaches and to provide a decision, suitable for the automotive applications.**

Keywords – **Gyroscope, MEMS, vibrating, analysis, technology**

I. INTRODUCTION

The gyroscope is a device that can measure angular velocity. This spinning device was being used on ships and aircrafts from 17th to 19th century, and in 20th century it was improved: optical gyroscope using laser was first invented and soon found commercial success in aeronautics and military applications. In the last ten to fifteen years, gyroscope microelectromechanical systems (GMEMS) have been introduced and their advantages over traditional macro-scale devices have been understood.

Nowadays, MEMS gyroscopes are used in a wide spectrum of areas: aerospace industry, military, medicine, automotive industry and consumer electronics market, with their reduced cost, size, and weight [1], [2], [3]. The consumer electronics applications include image stabilization in video cameras, virtual reality products, mobile phones, portable devices, MP3/MP4 players, PDAs, inertial pointing devices, computer gaming industry, etc. The automotive industry applications are diverse too, including high performance navigation and guidance systems, GPS receivers, ride stabilization, advanced automotive safety systems like yaw and tilt control, roll-over detection and prevention, and next generation airbag and anti-lock brake systems. The different usage of gyroscope MEMS supposes variety design solutions, according to the gyroscope type, design style, MEMS technology, actuation mechanism, coriolis sensor.

The aim at this paper is to investigate and discuss the kinds of angular gyroscope MEMS, to analyze approaches and to offer a decision for designing of gyroscope MEMS solution suitable for automotive applications.

K. Denishev, M. Nakova, I. Ivanov are with the Department of Microelectronics, Faculty of Electronic Engineering and Technologies, Technical University - Sofia, 8 Kliment Ohridski blvd., 1000 Sofia, Bulgaria, e-mail: khd@tu-sofia.bg

M. Ivanova is with the College of Energetics and Electronics, Technical University - Sofia, 8 Kliment Ohridski blvd., 1000 Sofia, Bulgaria, e-mail: m_ivanova@tu-sofia.bg

II. OPERATIONAL PRINCIPLE OF VIBRATORY GYROSCOPES

As above it was mentioned, there are an extensive variety of MEMS gyroscope designs, and operation principles exists, but almost all of the reported MEMS gyroscopes use vibrating mechanical elements to sense angular rate. The concept of utilizing vibrating elements to induce and detect Coriolis force involves no rotating parts that require bearings. Also, the vibrating elements are effectively implemented and batch fabricated in different micromachining processes.

The operation principle of the vast majority of all existing MEMS vibratory gyroscopes relies on the generation of a sinusoidal Coriolis force, due to the combination of vibration of a proof-mass and an orthogonal angular-rate input. The proof mass is generally suspended above the substrate by a suspension system, consisting of flexible beams [4]. The overall dynamical system is typically two degrees of freedom (DOF), (but nowadays there are with more, to 6-DOF) mass-spring-damper system, where the rotation induced Coriolis force causes energy transfer to the sense-mode, proportional to the angular rate input (Figure 1). In most of the reported MEMS vibratory rate gyroscopes, the proof mass is driven into resonance in the drive direction by an external sinusoidal electrostatic or electromagnetic force. For example (Figure 1), the proof-mass is driven into oscillation in the X-direction (drive mode) of the gyroscopic frame by the force F_d. When the proof-mass is subjected to an external rotation in the Z-direction, the induced Coriolis force causes the mass to oscillate in the Y-direction (sense mode). The magnitude of the sense oscillation is proportional to the rotation rate of the device.
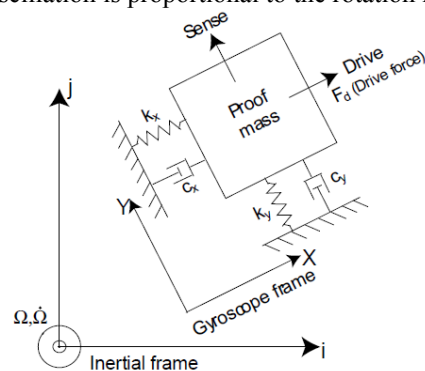

Figure 1. Operating principle of vibratory gyroscopes

When the gyroscope is subjected to an angular rotation, a sinusoidal Coriolis force is induced in the direction, orthogonal to the drive-mode oscillation at the driving

frequency. Ideally, it is desired to utilize resonance in both, the drive and the sense modes, in order to attain the maximum possible response gain. This is typically achieved by designing and electrostatically tuning the drive and sense resonant frequencies to match. The system from Figure 1 can be described with the following mathematical equations [5]:

Equation	Description
$\vec{r} = x.\vec{X} + y.\vec{Y}$	The position $\vec{r}$ of the mass m at any given time t in the gyroscope frame
$\dot{\vec{r}} = (\dot{x} - \Omega y)\vec{X} + (\dot{y} + \Omega x)\vec{Y}$	The induced velocity after rotation
$\ddot{\vec{r}} = (\ddot{x} - \Omega^2 x - 2\Omega\dot{y} - \dot{\Omega}y)\vec{X} + (\ddot{y} - \Omega^2 y - 2\Omega\dot{x} - \dot{\Omega}x)\vec{Y}$	The induced acceleration after rotation
$ma_x + c_x v_x + k_x x = F_d$ $ma_y + c_y v_y + k_y y = 0$, v – velocity, a-acceleration	The motion for the spring-mass-damper system with respect to the inertial frame
$m\ddot{x} + c_x \dot{x} + kx - 2m\Omega\dot{y} = F_d$ $m\ddot{y} + c_y \dot{y} + ky - 2m\Omega\dot{x} = 0$	The $2m\Omega\dot{y}$ and $2m\Omega\dot{x}$ are the items of the rotation induced Coriolis force

The $2m\Omega\dot{y}$ and $2m\Omega\dot{x}$ are the rotation induced Coriolis terms, which cause dynamic coupling between the two modes of vibration. When the stiffness values in the drive and the sense modes are matched, the resonant frequencies of the two modes are the same. If the system is then driven at its resonant frequency, the rotation induced Coriolis force excites the system into resonance in the sense direction. The resulting oscillation amplitude is proportional to the Coriolis force and therefore, to the angular velocity to be measured.

III. OVERVIEW AND ANALYSIS OF GYROSCOPE MEMS

In this section the different types of Gyroscope MEMS are discussed and as it seems over 2500 potential combinations for designing are possible (Figure 2).
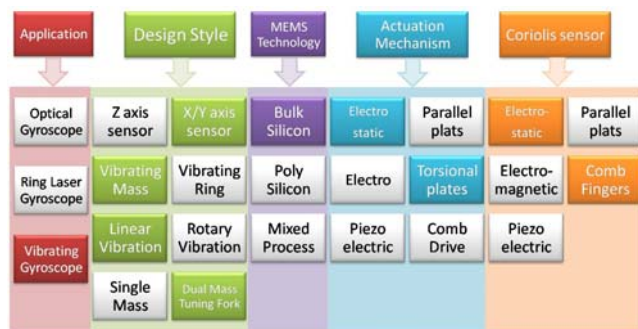

Figure 2. Over 2500 potential combinations for vibrating gyroscope MEMS

Gyroscopes are basically two high performing MEMS devices, integrated into one single device. They consist of a self-tuned resonator in the drive axis and a microgyroscope sensor in the sensing axis. The sensors are capacitive and they are used for measuring the small changes of capacitance. Gyroscope performance is very sensitive to all potential manufacturing variations, packaging, linear acceleration, temperature, etc. To achieve high performance and low cost, lots of care must be taken during the initial design. Gyroscope designers must achieve a solution that can be insensitive to most of these potential variations.

A. Gyroscope Types

In an optical gyroscope, lasers are typically used as the light source. Optical gyroscopes either employ straight line light paths with mirror surfaces or prisms at the edges to direct the light beam (a ring laser gyroscope) or a polarization glass – fiber loop (fiber optic gyroscopes - FOG). The glass fiber may actually loop multiple times, thus extending the effective length of the light path. The time delay between the clockwise and counterclockwise directions is detected by examining the phase interference between the clockwise and counterclockwise light signals. Multiple optical gyroscopes with nonparallel axes can be ganged together in order to measure three dimensional rotation. Various techniques can be used to measure the time difference between the two paths, including examining the Doppler (frequency) shift of the laser light due to the motion of the gyro and an examination of the beat frequency of the interference pattern between the clockwise and counterclockwise paths.

Fiber Optic Gyroscopes' fundamental principle is based on Sagnac effect who demonstrated detection of rotation with interference in light. A MEMS FOG system is proposed in [6]. The micromechanical technique is found to be suitable for creation of the nano-level light source and micro mirror and coupler. Such micro FOG system can be applied in the micro robot, unmanned air-vehicles, etc. The author mentions about one disadvantage of this method: the technology is being able to get large quantities of spider silk and it cannot be synthesized yet, and farming it is also impractical. The real system wants to be completed for several years.

A ring laser consists of a laser cavity in the shape of a ring. Light circulates in both directions around this cavity, producing two standing waves with the same number of nodes in both directions. Since the optical path lengths are different in the two directions, the resonant frequencies differ. The difference between these two frequencies is measured. An unfortunate side-effect of the ring-laser approach is that the two signals will lock in to each other for small rotation and it is typically necessary to physically rotate the device in a controlled manner in order to ensure that this lock in effect can be avoid [7].

So, the research shows that almost all MEMS gyroscopes are based on vibrating mechanical elements to sense rotation. Early MEMS gyroscopes utilized vibrating quartz crystals to generate the necessary linear motion. More recent designs have replaced the vibrating quartz crystals with silicon based vibrators.

B. GMEMS Design Styles

Bosch [8] has developed both *Z axis* and *X/Y axis* rate sensors. Its *Z axis* design was introduced in 1998 and uses

electromagnetic drive with capacitive sensing. Also, a *Z axis* copper gyroscope was developed by Carnegie Mellon University in 2002 [9]. It is fabricated through a CMOS process and has been designed to operate in normal atmospheric conditions.

The *X/Y-axis gyroscope* uses a rotary vibrating mass, it is typical for vibrating-wheel gyroscopes. It has a wheel that is driven to vibrate about its axis of symmetry, and rotation about either in-plane axis results in the wheel's tilting. The change can be detected with capacitive electrodes under the wheel. It is possible to sense two axes of rotation with a single vibrating wheel. A surface micromachined *polysilicon vibrating wheel gyroscope*, is designed at the U.C. Berkeley Sensors and Actuators Center [10].

The University of Michigan developed the first micromachined *vibrating ring gyroscope*. It was fabricated by electroforming nickel into a thick polyimide mold. This design was further enhanced by implementation in polysilicon using a high aspect ratio trench-fill technology [11].

At *linear vibration gyroscope* the moving mass is jointed with datum seat by flexible springs. The mass are only moved linearly in the direction of x-axis and y-axis due to the action of flexible supports and springs [12].

At the *MEMS gyroscopes with a single proof mass*, the proof mass is sustained by four springs and the motion is constrained along the x and y axis by making the spring stiffness of the z axis very large. Then, the proof mass can be modeled as a mass-spring-damper system with two degrees of freedom. The x axis is a drive axis, whose frequency is set to be identical with the resonant frequency of the drive mode. Coriolis acceleration, induced by z axis angular rate input and the linear acceleration input along y axis together induce the mass to oscillate along the y axis [13].

The Draper lab at MIT developed the first micromachined *tuning fork gyroscope* [14]. This gyroscope is fabricated using the SOI process. The tuning fork masses are electrostatically driven out-of-phase with comb-drives. The Coriolis response is measured by capacitance change due to the out-of-plane rocking mode.

At *X/Y axis dual-mass tuning fork gyroscope*, an angular velocity sensor has two masses, which are laterally disposed in an X/Y plane and indirectly connected to a frame. Angular velocity of the sensor about the y axis can be sensed by driving the two masses into z directed antiphase oscillation. The measuring of the angular oscillation amplitude thereby imparted to the frame.

C. GMEMS Technology

An example of *bulk micromachining process* is reported in [15], where a lateral-axis vibratory gyroscope that has both single-crystal silicon microstructures and full CMOS - compatibility is presented. The DRIE silicon post-CMOS micromachining process flow and a fabricated example microstructure are shown in Figure 3. The steps are as follows: (1) a backside DRIE silicon etch is performed (i), (2) a front-side reactive-ion etch of the dielectric layers forms structural sidewalls masked by the top CMOS metal layer (ii), (3) another DRIE silicon etch extends the structural sidewalls into the underlying silicon (iii), (4) a

short timed isotropic silicon etch (iv)] which provides a specific undercut of the exposed silicon sidewalls.
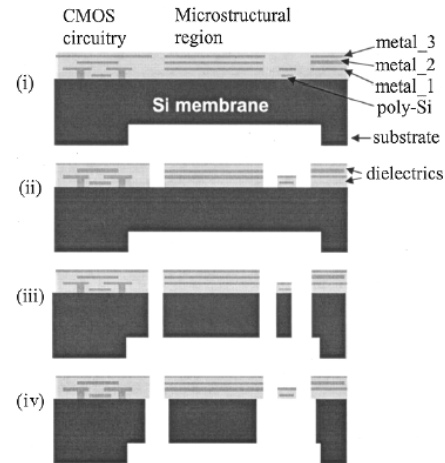

Figure 3. Bulk machining DRIE CMOS-MEMS process

In a standard three polysilicon layer *surface micromachining process* [16], the moving parts of the device are formed, using the second structural polysilicon layer (Poly1) or the third (Poly2). The electrical connections are formed using the first structural polysilicon layer (Poly0) deposited on the nitride-covered substrate. The steps of the process are as follows (Figure 4): (1) deposition of a 600 nm low-stress Silicon Nitride layer on the silicon n-type (100) wafers as an electrical isolation layer, after this the deposition of the first structural polysilicon film Poly0 is performed; (2) Poly0 is photolithographycally patterned: the Poly0 layer is first coated with photoresist, then, photoresist is exposed with the first level mask (Poly0), and the exposed photoresist is developed to create the desired etch mask for subsequent pattern transfer to the underlying layer; (3) After patterning the photoresist, the uncovered areas of the Poly0 layer is etched in an RIE (Reactive Ion Etch) system, the remaining photoresist is stripped away; (4) A 2.0 μm phosphosilicate glass (PSG) sacrificial layer is then deposited by LPCVD, this sacrificial layer of PSG, known as the Oxide layer, is removed at the end of the process to free the first mechanical layer of polysilicon; (5) The sacrificial layer is lithographically patterned with the dimples mask and the dimples are transferred into the sacrificial PSG layer by RIE, the wafers are then patterned with the third mask layer, the anchor mask, and reactive ion etched. This step provides anchor holes that will be filled by the second polysilicon layer (Poly1);
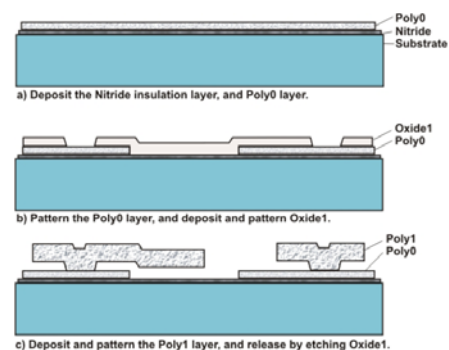

Figure 4. The process flow of a standard surface-micromachining process

(6) After etching anchors, the second structural layer of polysilicon is deposited, this structural layer has a thickness of 2.0 μm, and the moving structures including the proof mass, suspension system and the capacitors are formed in this layer; (7) The polysilicon is lithographically patterned using a mask designed to form the second structural layer Poly1, after etching the polysilicon, the photoresist is stripped.

The same procedure is followed to form the second sacrificial layer Oxide2 and the third structural layer Poly2.

Recently, the *mixed micro-machining process* which has the merits of a conventional surface and bulk micro-machining process on a single crystal silicon is applied in GMEMS design (Figure 5). The included processes at this technology are: single crystal reactive etching and metallization, silicon micromachining by plasma etching, silicon on insulator, surface/bulk micromashining process, reverse surface micromachining process. These micromachining techniques applied to bulk silicon have allowed the designer to form three dimensional microstructiures that can be moved lateral of vertical to the plane of the device [17].
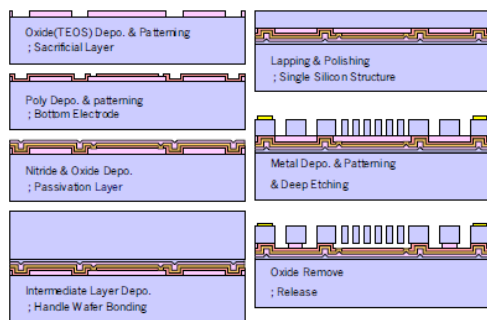

Figure 5. Steps of mixed technology process

IV. CONCLUSION AND FUTURE WORK

In the paper an investigation of GMEMS is presented, according to operational principles, design styles and technologies. It points to a wide variety of design solutions–over 2500 potential combinations. The detailed exploration shows that in the automotive sector, the gyroscope MEMS are applied for rollover detection, in GPS navigation electronic stability control (ESC) and adaptive cruise control (ACC). Such applications require wide bandwidth frequency responses in the drive and sense modes and precise sensibility. Despite of the different realized solutions of GMEMS, the design approaches are in their immature phase and they are in the research scope of scientific teams. The performed analysis of GMEMS in this paper is used for decision making about angular GMEMS design that will be performed in our future activities: z axis gyroscope, with a vibrational lumped mass-spring system, with electrostatic combs used for drive and sense.

AKNOWLEDGMENT

REFERENCES

[1] J. Bouchaud. *MEMS Industry and Market Overview*, 2008, http://www.uclouvain.be/cps/ucl/doc/chairemems/documents/MEMS_market_louvain_wtc.pdf

[2] Nanotechnology Group, *Micro-electro-mechanical Systems,* http://knowledgecontext.org/COSMOS/Kubby_MEMS_2007.pdf

[3] D. Wicaksono, Y. Chen, P. French. *Design and Modelling of a Bio-inspired MEMS Gyroscope*, Proceedings of the International Conference on Electrical Engineering and Informatics Institut Teknologi Bandung, Indonesia, June 17-19, 2007.

[4] J. Geen, D. Krakauer. *New iMEMS Angular-Rate-Sensing Gyroscope*, 2003, http://www.analog.com/library/analogDialogue/archives/37-03/gyro.pdf

[5] X. Li, R. Lin, K. Leow. *Performance-Enhanced Micro-Machined Resonant Systems with Two-Degrees-of-Freedom Resonators*, Journal of Micromech,Microengineering, vol. 10, 2000, pp. 534-539.

[6] B. Zhang. Overview and Improving Fiber Optic Gyroscope Based on MEMS/NEMS Fabrication, 2006, http://www.iop.org/EJ/article/1742-6596/34/1/025/jpconf6_34_025.pdf?request-id=d829c17a-1bd2-49f3-9f20-50246763842a

[7] J. Sharp. Laser Gyroscopes, http://www.mech.gla.ac.uk/~sharpj/lectures/lasers/notes/laser_gyro.pdf

[8] P. Ernst, R. Bosch. *MEMS@BOSCH: Automotive applications and beyond*, Automotive Electronics, http://www.mstbw.de/imperia/md/content/mstbw/bestpractice/bosch_mems_12_micromachine_symposium_ernst.pdf

[9] H. Luo, X. Zhu, H. Lakdawala, L. Carley, G. K. Fedder. *A copper CMOS- MEMS z-axis gyroscope*, 15th IEEE Int. Conf. Microelectromechanical Systems, Las Vegas, pp. 631-634, 2001.

[10] Berkeley Sensor & Actuator Center, http://www-bsac.eecs.berkeley.edu/

[11] F. Ayazi, K. Najafi. *Design and fabrication of a high performance polysilicon vibrating ring gyroscope*, IEEE Micro Electromechanical Systems Workshop, Heidelberg, Germany, pp. 621-626, 1998.

[12] G. Qiufen, G. Yuansheng, S. Feng, L. Fuqiang. *Gas Damping Coefficient Research For The Mems Comb Linear Vibration Gyroscope*, DTIP 2007, Stresa, Maggiore : Italy, 2007, http://hal.archives-ouvertes.fr/docs/00/25/76/97/PDF/dtip07_1034.pdf

[13] W. Sung, T. Kang, J. Lee. *Controller Design of a MEMS Gyro-Accelerometer with a Single Proof Mass*, International Journal of Control, Automation, and Systems, vol. 6, no. 6, pp. 873-883, 2008, http://www.ijcas.org/admin/paper/files/IJCAS_v6_n6_pp.873-883.pdf

[14] J. Bernstein, S. Cho, A. King, A. Kourepenis, P. Maciel, M.Weinberg. *A micromachined comb-drive tuning fork rate gyroscope*, IEEE Microelectromechanical Systems, Fort Lauderdale, FL, pp. 143-148, 1993.

[15] H. Xie, G. Fedder, A CMOS-MEMS lateral-axis Gyroscope, http://www.ece.cmu.edu/~mems/pubs/pdfs/ieee/mems/0032_xie-2001.pdf

[16] D. Koester, R. Mahadevan, B. Hardy, K. Markus. *MUMPs Design Handbook*, Cronos Integrated Microsystems, 2000.

[17] B. Lee, S. Lee, K. Jung, J. Choi, T. Chung, Y. Cho. *A decoupled vibratory gyroscope using a mixed micro-machining technology*, IEEE International Conference on Robotics & Automation, Seoul, Korea, 2001, http://www.ent.mrt.ac.lk/iml/paperbase/ICRA_CDs/ICRA2001/PDFFILES/PAPERS/ICRA_PAPERS/Z1078.pdf